On the non ideality of CO_2 solutions in ionic liquids and other low volatile solvents

Pedro J. Carvalho and João A. P. Coutinho

CICECO, Departamento de Química, Universidade de Aveiro, 3810-193, Aveiro, Portugal

The non ideality of CO_2 solutions in non volatile solvents:

To analyze the non ideality of CO_2 solutions in non volatile solvents, experimental VLE data at subcritical and near critical conditions for a wide range of systems, comprising alcohols, alkanes fatty acids, fatty acid esters, PEGs, and ionic liquids, was compared with the solubilities predicted by the Raoult's law (manuscript eq. (1)) described as

$$P = x_{CO_2} \gamma_{CO_2} P^{\sigma}_{CO_2} \quad (1)$$

where $\gamma_{CO2}=1$ is the CO_2 activity coefficient and P^{σ}_{CO2} the vapor pressure of CO_2, determined using DIPPR information and data evaluations manager for the vapor pressure of liquid CO_2

$$P^{\sigma}_{CO_2}(Pa) = e^{140.54 - \frac{4735}{T/K} - 21.268 \ln(T/K) + 0.040909 \; T/K} \quad (2)$$

In the analysis of the other systems it must be recalled that the non-ideality results not only from differences in the energetic interactions between the molecules, as described by the residual contribution to the Gibbs free energy, but also from entropic effects due to their size and shape differences, the combinatorial contribution, as summarized by

$$G^E = G^E_{comb} + G^E_{residual} \quad (3)$$

The entropic effects will always have a negative contribution to the non-ideality that in terms of activity coefficients can be described by the Flory-Huggins equation

$$\ln\left(\gamma_{CO_2}^{comb}\right) = \ln\frac{\varphi_{CO_2}}{x_{CO_2}} + \left(1 - \frac{\varphi_{CO_2}}{x_{CO_2}}\right) \quad (4)$$

where $\varphi_{CO_2} = x_{CO_2} V_{CO_2} \Big/ \sum_i x_i V_i$ is the volume fraction and V_i are the molar volumes of the various compounds present in the mixture.

If the combinatorial contributions to the non-ideality alone are taken into account the Eq. (1) will become

$$P = x_{CO_2} \exp\left\{\ln\frac{\varphi_{CO_2}}{x_{CO_2}} + \left(1 - \frac{\varphi_{CO_2}}{x_{CO_2}}\right)\right\} P_{CO_2}^{\sigma} \quad (5)$$

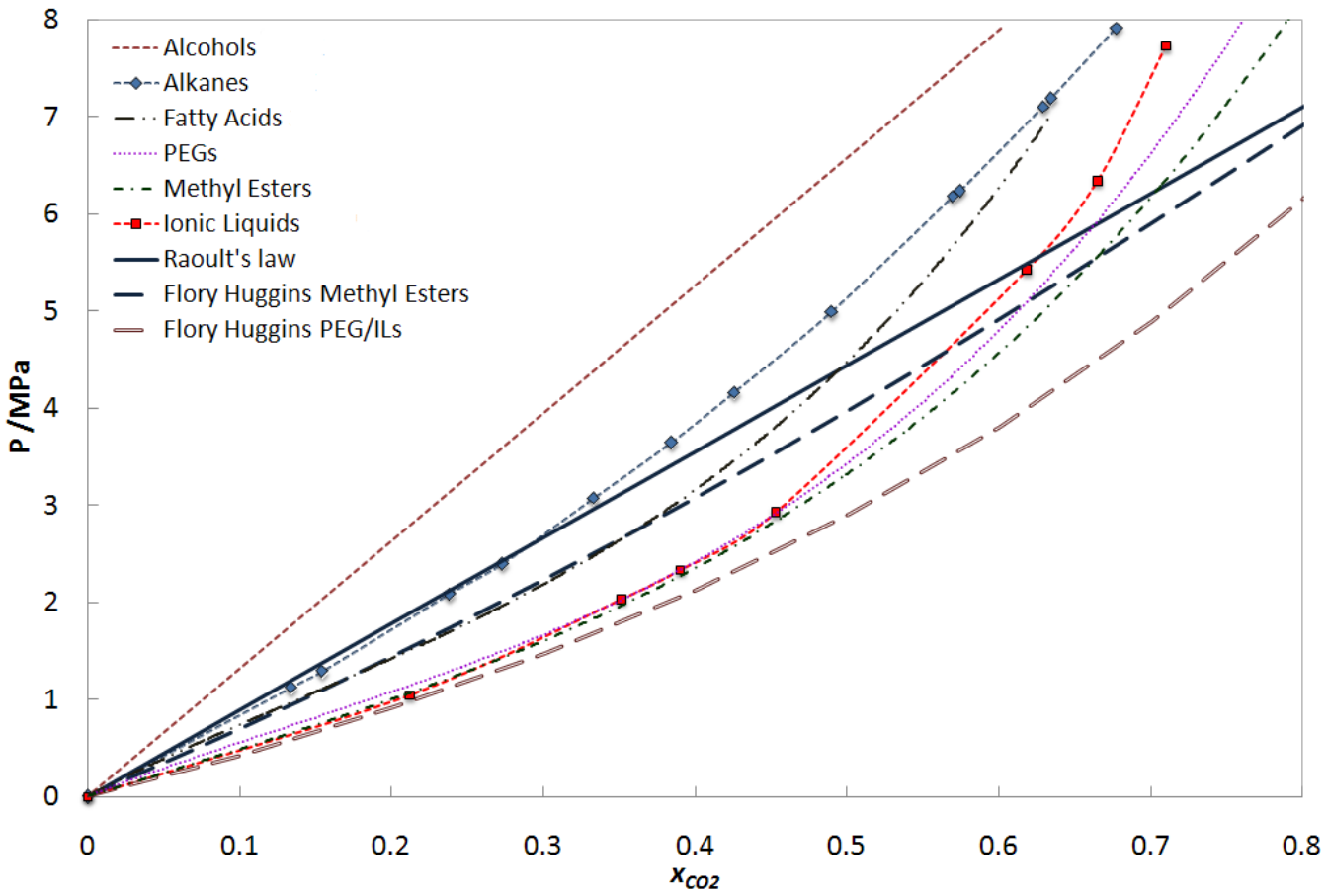

Figure 1a. *(manuscript Figure 1)* Sketch of the pressure - CO_2 molar composition diagram for the systems CO_2 + Alcohols, CO_2 + Alkanes, CO_2 + Fatty acids, CO_2 + PEGs, CO_2 + Fatty acid esters, and , CO_2 + Ionic liquids at 313 K.

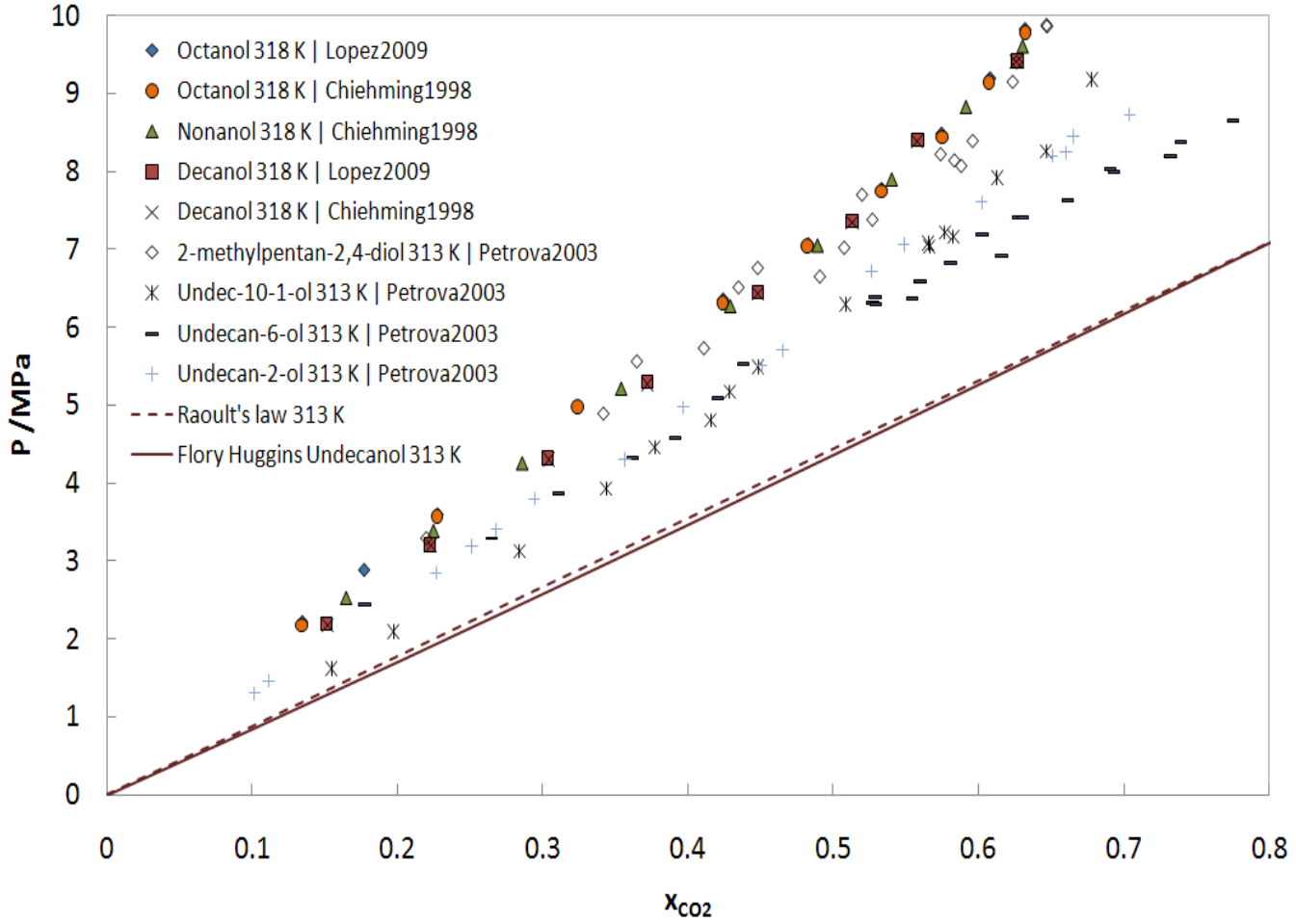

Fi**gure 1b.** Pressure - CO_2 molar composition diagram for the systems CO_2 + Alcohols at 313 K.[3-5]

In spite of the stability of the CO_2-OH EDA complexes observed spectroscopically[1;2] the alcohol containing systems are the only with positive deviations to ideality as sketched in Figure 1a and depicted in Figure 1b.

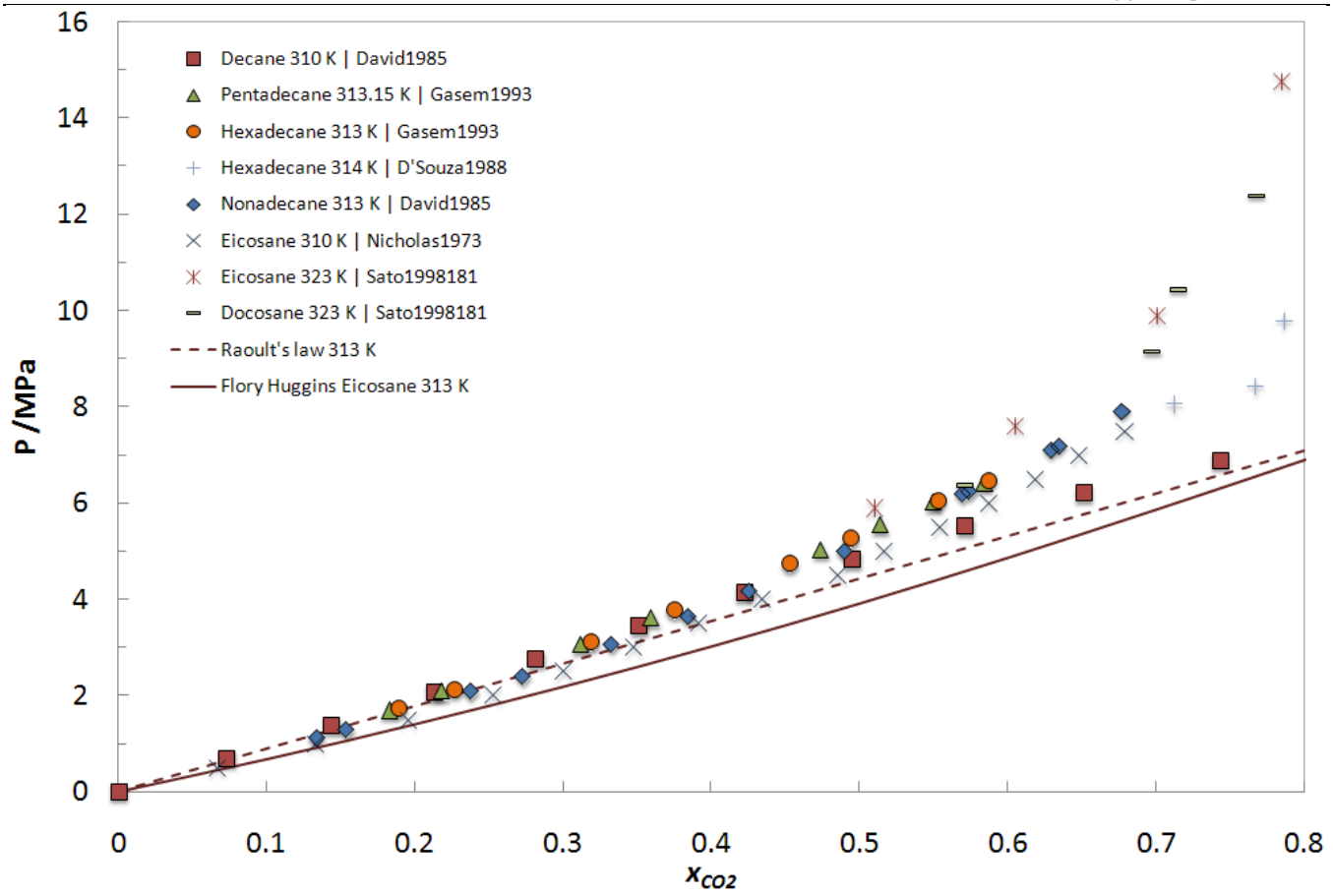

Fi**gure 1c.** Pressure - CO_2 molar composition diagram for the systems CO_2 + Akanes at 313 K.[6-10]

The pressure *vs*. mol fraction plot of the CO_2 solubility in alkanes sketched in Figure **1c** shows a behavior very close to the ideal behavior described by Raoult's law. Given the negative deviations to ideality predicted by the Flory-Huggins model for these systems the near ideal behavior must result from positive deviations in the residual (enthalpic) term. These arise from CO_2-alkane interactions that must be weaker than the CO_2-CO_2 or alkane-alkane interactions.

Both fatty acids and PEGs show a non-ideal behavior than can be well described by the Flory-Huggins equation while the esters display the largest deviations to the ideal behavior observed for all the systems studied as shown in Figures 1a, 1d and 1e. For these systems the Electron Donor-Acceptor complexes formed between CO_2 and the carbonyl group, though not stronger than those formed with the hydroxyl groups of alcohols are favored as the CO_2-carbonyl interactions seem to be energetically favorable when compared with the CO_2-CO_2 interactions and the carbonyl-carbonyl interactions established between the ester molecules.

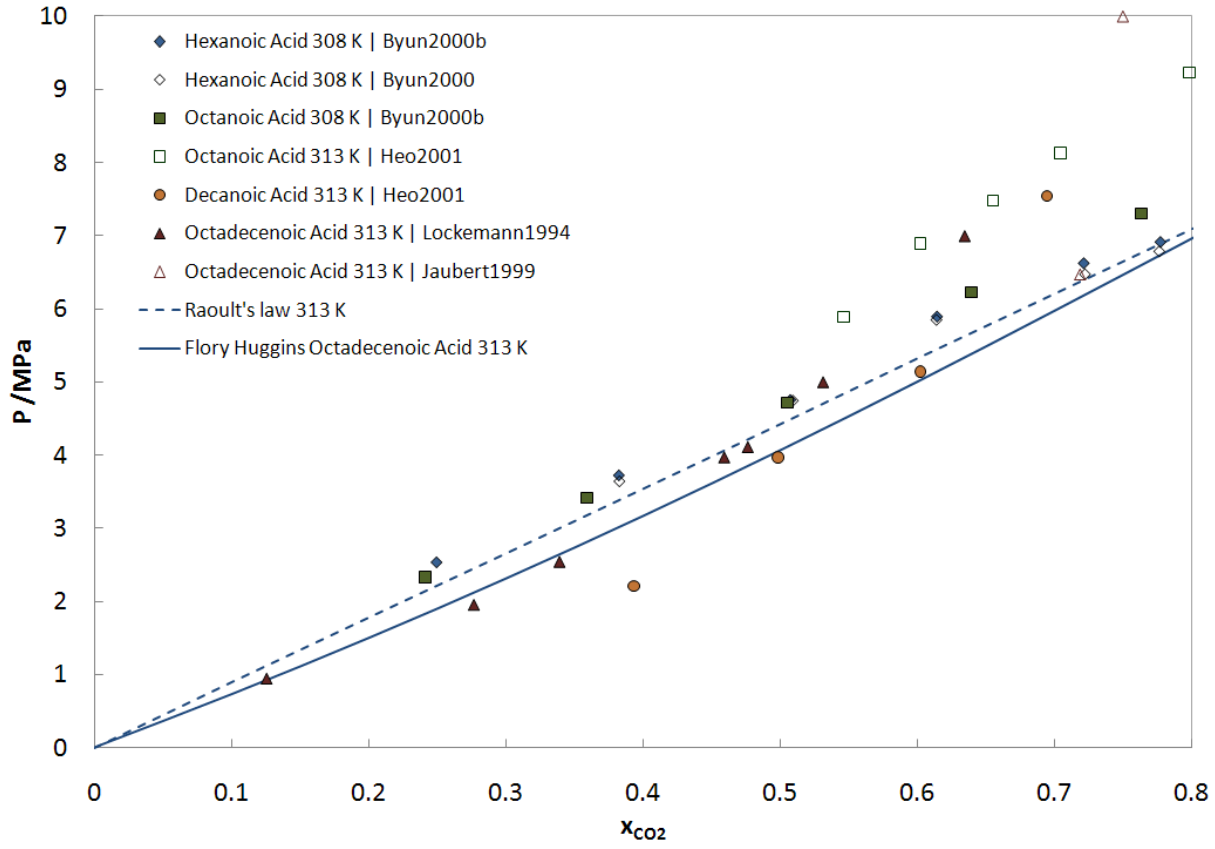

Fi**gure 1d.** Pressure - CO_2 molar composition diagram for the systems CO_2 + Fatty acids at 313 K.[11-16]

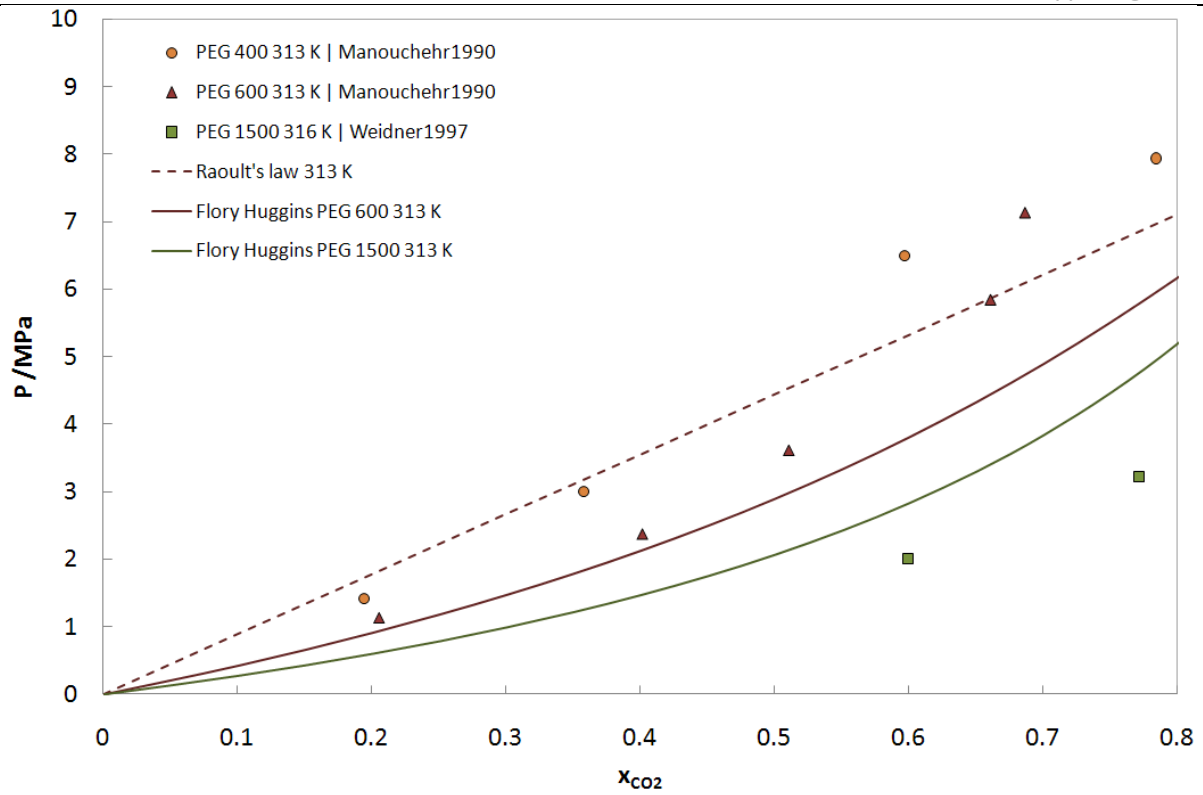

Figure 1e. Pressure - CO_2 molar composition diagram for the systems CO_2 +PEGs at 313 K.[17;18]

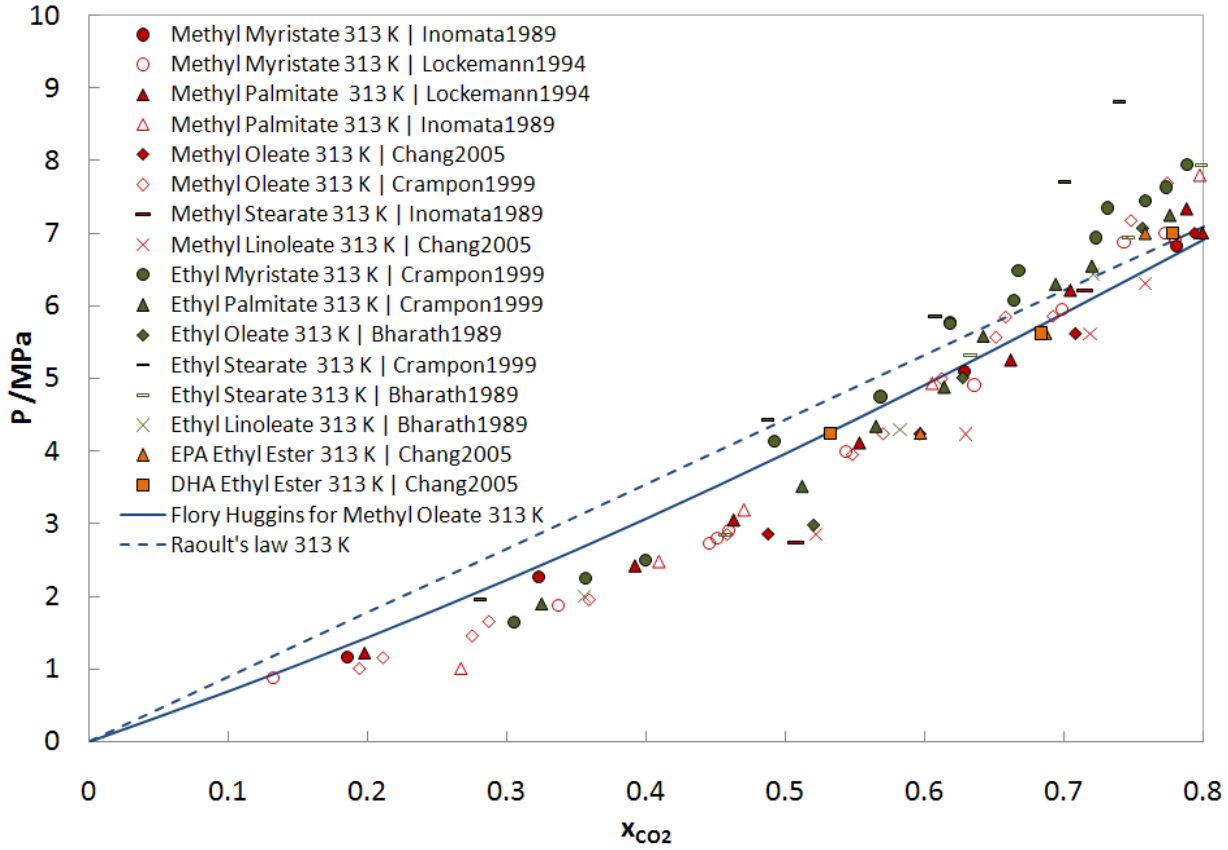

Figure 1f. Pressure - CO_2 molar composition diagram for the systems CO_2 + Fatty acid esters at 313 K.[11;12;19-21]

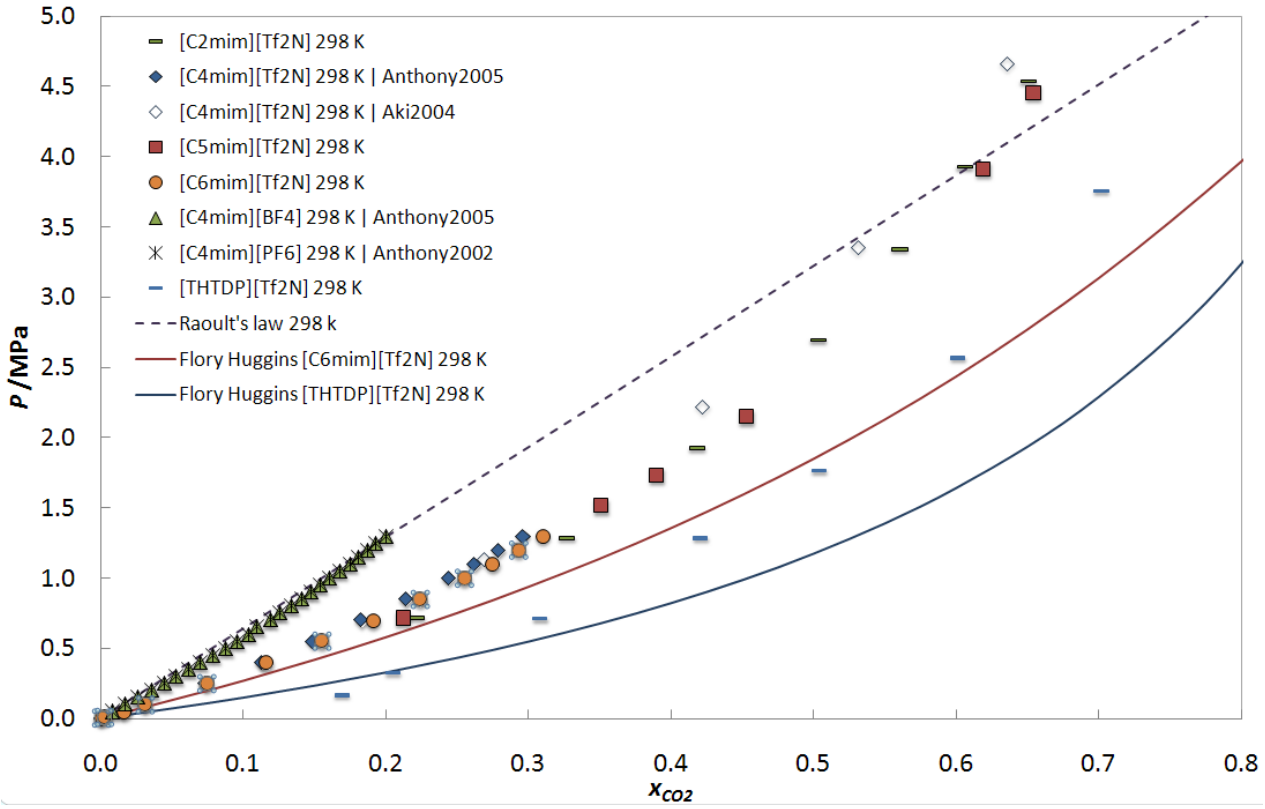

Figure 1g. Pressure - CO_2 molar composition diagram for the systems CO_2 + Ionic Liquids at 313 K.[22-27]

[THTDP][Cl] Experimental measurements:

The high pressure equilibrium cell developed uses the synthetic method and is sketched in Figure 2. The cell, based on the design of Daridon et al.[28-32], consists of a horizontal hollow stainless-steel cylinder, closed at one end by a movable piston and at the other end by a sapphire window. This window, along with a second window on the cell wall through which an optical fiber lights the cell chamber, allows the operator to follow the behavior of the sample with pressure and temperature. The orthogonal positioning of both sapphire windows minimizes the parasitic reflections and improves the observation in comparison to axial lighting.

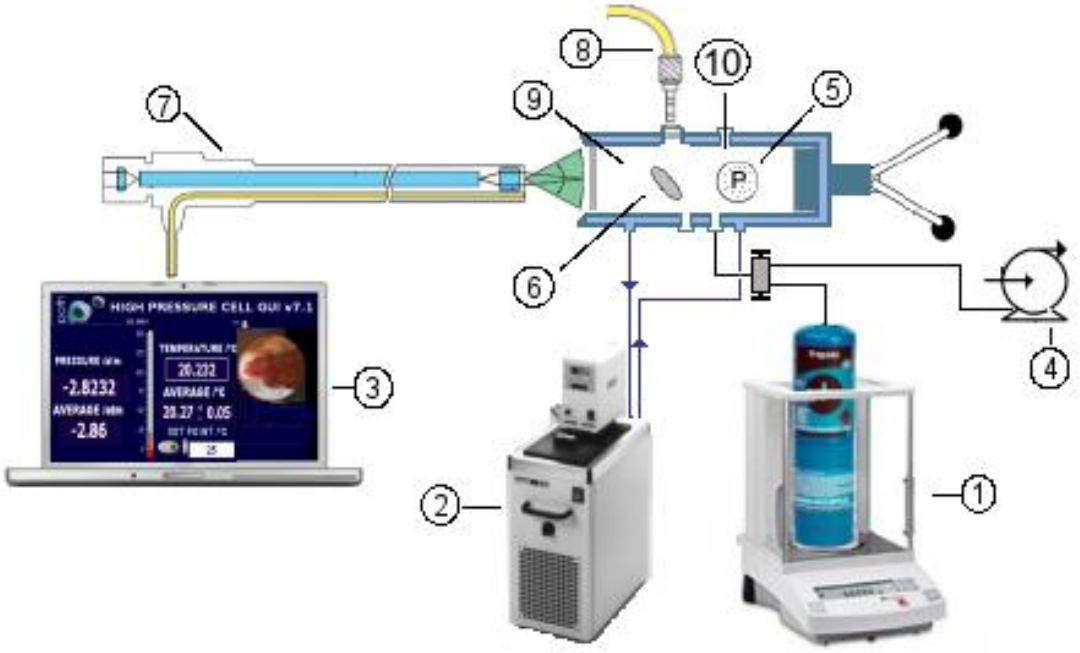

Figure 2. Schematic apparatus: 1 – Analytical balance (Sartorius LA200P); 2 – Thermostatized bath circulator (Julabo MC); 3 – Computer for data and video acquisition; 4 – Vacuum pump (Edwards RV3); 5 – Piezoresistive pressure transducer (Kulite HEM 375); 6 – Magnetic bar; 7 – Endoscope plus a video camera; 8 – Light source with optical fiber cable; 9 – High-pressure variable-volume cell; 10 – Temperature probe (K type thermocouple).

A small magnetic bar placed inside the cell allows the homogenization of the mixture by means

of an external magnetic stirrer. The sapphire window on the cell wall limits the minimum internal volume of the cell to 8 cm^3, while the maximum value is set to 30 cm^3. The presence of the magnetic stirrer, as well as the cell reduced volume, help to minimize the thermal inertia and temperature gradients within the sample.

The cell is thermostatized by circulating a heat-carrier fluid through three flow lines directly managed into the cell. The heat-carrier fluid is thermo-regulated with a temperature stability of ±0.01 K by means of a thermostat bath circulator (Julabo MC). The temperature is measured with a high precision thermometer, Model PN 5207 with an accuracy of 0.01 K, connected to a calibrated platinum resistance inserted inside the cell close to the sample. The pressure is measured by a piezoresistive silicon pressure transducer (Kulite) fixed directly inside the cell to reduce dead volumes, that was previously calibrated and certified by an independent laboratory with IPAC accreditation, following the EN 837-1 standard and with accuracy better than 0.2%.

A fixed amount of IL was introduced inside the cell, its exact mass was determined by weighting, using a high weight/high precision balance with an accuracy of 1 mg (Sartorius). In order to avoid any interference of atmospheric gases during the manipulation, after placing the IL inside the cell, it was kept under vacuum overnight, while stirring and heating at 353 K.

The CO_2 was introduced under pressure from an aluminum reservoir tank. Its mass was measured with the precision balance and introduced into the measuring cell by means of a flexible high pressure capillary.

After preparation of a mixture of known composition and the desired temperature at low pressure was reached, the pressure was then slowly increased at constant temperature until the system becomes monophasic. The pressure at which the last bubble disappears represents the equilibrium pressure for the fixed temperature.

The purity of the IL is re-checked by NMR at the end of the study to confirm that no degradation of the IL takes place during the measurements.

The tetradecyltrihexylphosphonium chloride, [THTDP][Cl], was provided by Cytec with mass fraction purities higher than 97 %. The supplier reports the existence of tetradecene isomers (0.1 to 0.4 %) and 0.1 to 0.5 % of HCl and thus a purification procedure was applied prior to the measurements. The [THTDP][Cl] was repeatedly washed with ultrapure water, the water rich phase removed and the IL dried under vacuum (0.1 Pa), stirring and moderate temperature (353 K). The final water content was determined with a Metrohm 831 Karl Fischer coulometer, indicating a water mass fraction of $269 \cdot 10^{-6}$.

The carbon dioxide (CO_2) was acquired from Air Liquide with a purity of ≥ 99.998 % and H_2O, O_2, C_nH_m, N_2 and H_2 impurities volume fractions lower than (3, 2, 2, 8 and 0.5)$\cdot 10^{-6}$, respectively.

The results obtained are reported in Table 1.

Table 1. Bubble point data of the system CO_2 (1) + [THTDP][Cl] (2).

x_1	P /MPa	x_1	P /MPa	x_1	P /MPa	x_1	P /MPa
313 K				363 K			
0.119	0.168	0.503	2.850	0.119	0.770	0.503	5.692
0.164	0.371	0.603	4.135	0.164	1.089	0.603	8.330
0.200	0.517	0.701	6.130	0.200	1.397	0.701	12.821
0.305	1.120	0.752	7.503	0.305	2.440	0.752	16.927
0.400	1.824	0.800	16.31	0.400	3.679	-	-

Manuscript Figure 2:

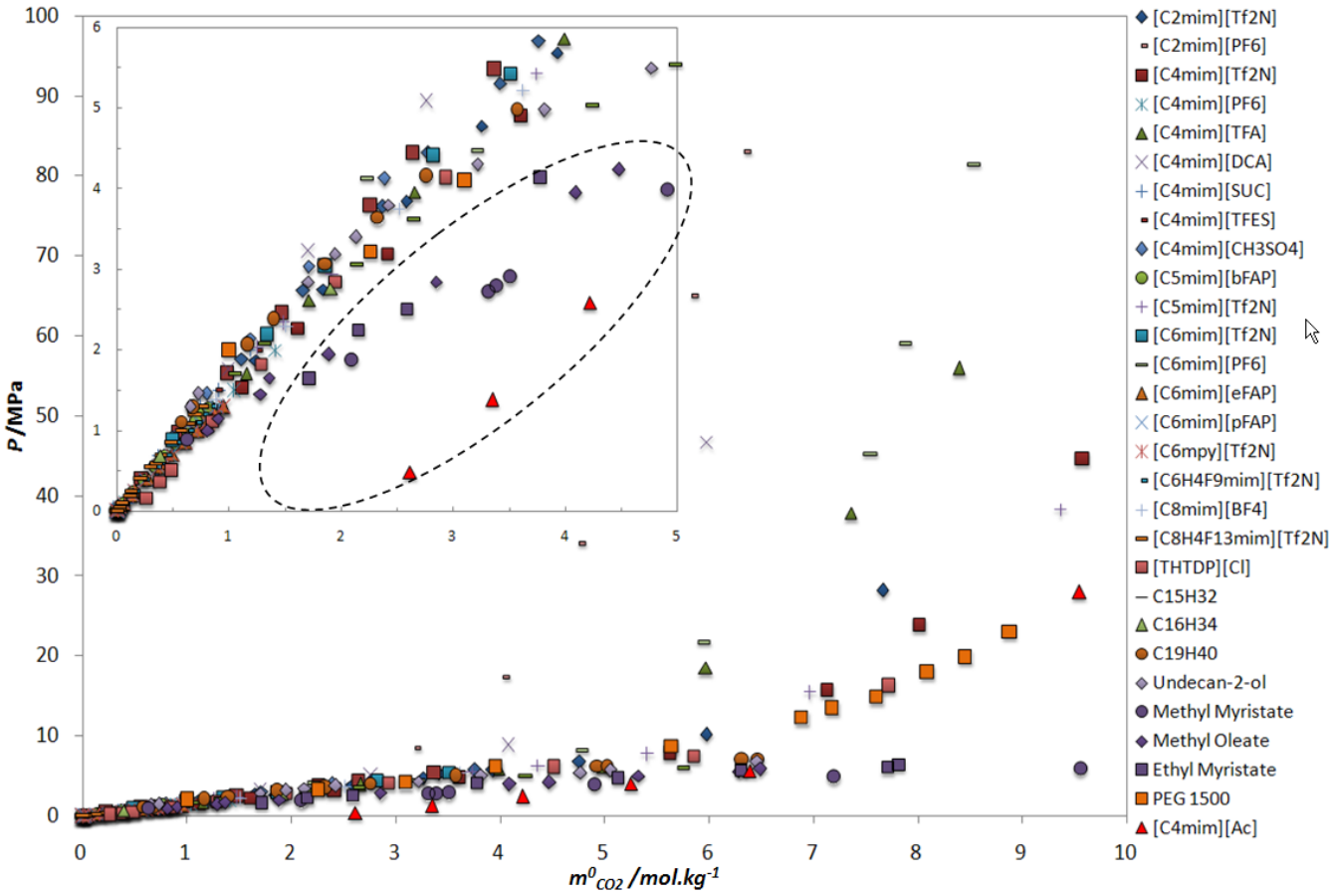

Figure 3. *(Figure 2 in manuscript)* Pressure - molality diagram of CO_2 + non volatile solvents at 313 K. Data from manuscript Refs. [12;13;16;17;23;26;31;48;78-84].

Figure 3 represents, on a p-m diagram at 298 K, the solubility of CO_2 in a large number of ionic liquids, listed in Table 8, along with the solubility of CO_2 in various other solvents. Data from manuscript Refs. [12;13;16;17;23;26;31;48;78-84]..

Table 2. List of ionic liquids depicted in Figure 3.

$[C_2mim][Tf_2N]$	1-ethyl-3-methylimidazolium bis(trifluoromethylsulfonyl)imide[22,39]
$[C_4mim][Tf_2N]$	1-butyl-3-methylimidazolium bis(trifluoromethylsulfonyl)imide[23]
$[C_5mim][Tf_2N]$	1-methyl-3-pentylimidazolium bis(trifluoromethylsulfonyl)imide[22]
$[C_6mim][Tf_2N]$	1-hexyl-3-methylimidazolium bis(trifluoromethylsulfonyl)imide[37]
$[C_4mim][BF_4]$	1-butyl-3-methylimidazolium tetrafluoroburate[34]
$[C_8mim][BF_4]$	1-octyl-3-methylimidazolium tetrafluoroburate[40]
$[C_2mim][PF_6]$	1-ethyl-3-methylimidazolium hexafluorophosphate[41]
$[C_4mim][PF_6]$	1-butyl-3-methylimidazolium hexafluorophosphate[3438]
$[C_6mim][PF_6]$	1-hexyl-3-methylimidazolium hexafluorophosphate[41]
$[C_4mim][TFA]$	1-butyl-3-methylimidazolium trifluoroacetate[33]
$[C_4mim][DCA]$	1-butyl-3-methylimidazolium dicyanamide[23]
$[C_4mim][SUC]$	1-butyl-3-methylimidazolium succinamate[34]
$[C_4mim][TFES]$	1-butyl-3-methylimidazolium tetrafluoroethanesulfonate[34]
$[C_4mim]_2[IDA]$	bis(1-butyl-3-methylimidazolium).iminodiacetate[34]
$[C_5mim][Tf_2N]$	1-methyl-3-pentylimidazolium bis(trifluoromethylsulfonyl)imide[22]
$[C_5mim][bFAP]$	1-methyl-3-pentylimidazolium tris(nonafluorobutyl)trifluorophosphate[35]
$[C_6mim][Tf_2N]$	1-hexyl-3-methylimidazolium bis(trifluoromethylsulfonyl)imide[34]
$[C_6mim][eFAP]$	1-hexyl-3-methylimidazolium tris(pentafluoroethyl)trifluorophosphate[35]
$[C_6mim][pFAP]$	1-hexyl-3-methylimidazolium tris(heptafluoropropyl)trifluorophosphate[35]
$[C_6mpy][pFAP]$	1-hexyl-3-methylpyridinium tris(heptafluoropropyl)trifluorophosphate[35]
$[C_6mpy][Tf_2N]$	1-hexyl-3-methylpyridinium bis(trifluoromethylsulfonyl)imide
$[C_6H_4F_9mim][Tf_2N]$	1-methyl-3-(nonafluorohexyl)imidazolium bis(trifluoromethylsulfonyl)imide[35]
$[C_8H_4F_{13}mim][Tf_2N]$	1-methyl-3-(tridecafluorooctyl)imidazolium bis(trifluoromethylsulfonyl)imide[35]
[TBP][FOR]	tetra-n-butylphosphonium formate[34]
[THTDP][Cl]	trihexyltetradecylphosphonium chloride[24]
$[C_4mim][CH_3SO_4]$	1-butyl-3-methylimidazolium methyl sulfate[38]
$[C_4mim][Ac]$	1-butyl-3-methylimidazolium acetate [31]

Manuscript Figure 3:

For pressures up to 10 MPa the fugacity of CO_2 is proportional to the system pressure and can be described by

$$p = H_i m_i^o \quad (6)$$

where H_i combines the Henry's constant, $k_{H,i}^{(m)}$, with the gas phase non ideality, proportional to pressure, and the liquid phase non ideality, proportional to concentration.

The best description of the Henry's constant temperature dependence is provided by Benson and Krause,[43;44] and within a temperature range of 100 K can be expressed as

$$\ln H_i = \alpha + \frac{\beta}{T} \quad (7)$$

Combining Eqs. (1) and (2) it is possible to develop a general description for the solubility of CO_2 in non volatile solvents. For this purpose experimental data from various authors and various types of non volatile solvents was used. This data was retrieved from the references [12;13;16;23;31;81] of the manuscript. The result is shown in Figure 4 where the value of H_i at each temperature is reported.

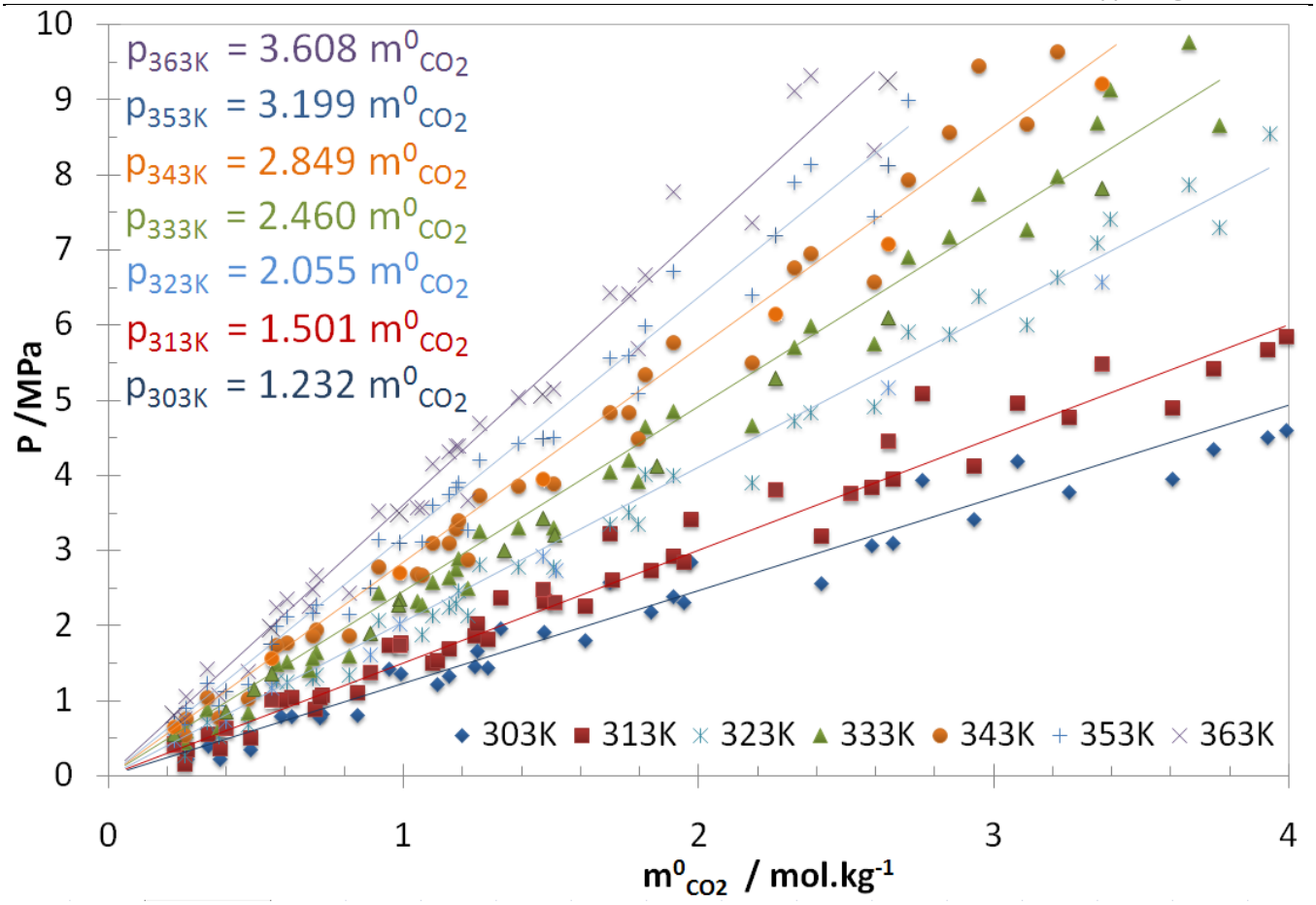

Figure 4. Pressure - molality diagram of CO_2 + non volatile solvents. Data from the references [12;13;16;23;31;81] of the manuscript.

The correlation of Eq. (2) to the Henry's constants reported in Figure 4 is depicted in Figure 5

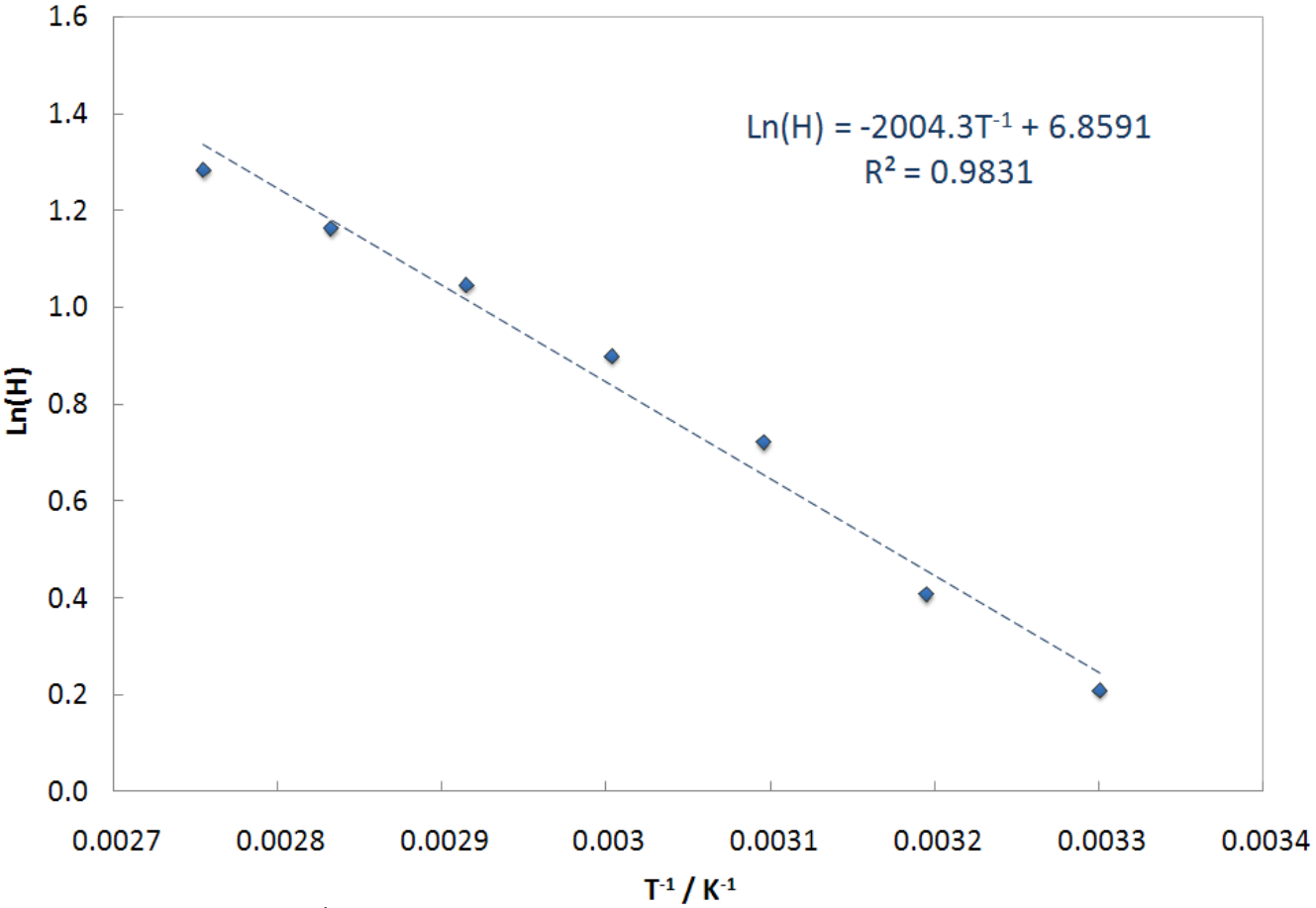

Figure 5. Ln(H) *versus* T^{-1} of CO_2 + non volatile systems depicted in Figure 4.

Literature Cited

(1) Lalanne, P.; Tassaing, T.; Danten, Y.; Cansell, F.; Tucker, S. C.; Besnard, M. CO_2-Ethanol Interaction Studied by Vibrational Spectroscopy in Supercritical CO_2. *J. Phys. Chem. A* **2004**, 108, 2617-2624.

(2) Fulton, J. L.; Yee, G. G.; Smith, R. D. Hydrogen Bonding of Methyl Alcohol-D in Supercritical Carbon Dioxide and Supercritical Ethane Solutions. *J. Am. Chem. Soc.* **1991**, 113, 8327-8334.

(3) López, J. A.; Trejos, V. M.; Cardona, C. A. Parameters Estimation and VLE Calculation in Asymmetric Binary Mixtures Containing Carbon Dioxide + N-Alkanols. *Fluid Phase Equilib.* **2009**, 275, 1 - 7.

(4) Chang, C. J.; Chiu, K.; Day, C. A New Apparatus for the Determination of P-X-y Diagrams and Henry's Constants in High Pressure Alcohols With Critical Carbon Dioxide. *J. Supercrit. Fluids* **1998**, 12, 223 - 237.

(5) Petrova, E.; Crampon, C.; Ali, E.; Neau, E.; Badens, E.; Charbit, G.; Jaubert, J. N. Solubility of CO2 in Some Heavy Alcohols and Correlation of Fluid Phase Equilibrium. *Fluid Phase Equilib.* **2003**, 213, 153 - 162.

(6) Fall, D. J.; Fall, J. L.; Luks, K. D. Liquid-Liquid-Vapor Immiscibility Limits in Carbon Dioxide + N-Paraffin Mixtures. *J. Chem. Eng. Data* **2002**, 30, 82-88.

(7) Tanaka, H.; Yamaki, Y.; Kato, M. Solubility of Carbon Dioxide in Pentadecane, Hexadecane, and

Pentadecane + Hexadecane. *J. Chem. Eng. Data* **1993**, 38, 386-388.

(8) Sato, Y.; Tagashira, Y.; Maruyama, D.; Takishima, S.; Masuoka, H. Solubility of Carbon Dioxide in Eicosane, Docosane, Tetracosane, and Octacosane at Temperatures From 323 to 473 K and Pressures Up to 40 MPa. *Fluid Phase Equilib.* **1998**, 147, 181-193.

(9) Huie, N. C.; Luks, K. D.; Kohn, J. P. Phase-Equilibriums Behavior of Systems Carbon Dioxide-N-Eicosane and Carbon Dioxide-N-Decane-N-Eicosane. *J. Chem. Eng. Data* **1973**, 18, 311-313.

(10) D'souza, R.; Patrick, J. R.; Teja, A. S. High Pressure Phase Equilibria in the Carbon Dioxide - *n*-Hexadecane and Carbon Dioxide - Water Systems. *Can. J. Chem. Eng.* **1988**, 66, 319-323.

(11) Lockemann, C. A. High-Pressure Phase Equilibria and Densities of the Binary Mixtures Carbon Dioxide--Oleic Acid, Carbon Dioxide--Methyl Myristate, and Carbon Dioxide--Methyl Palmitate and of the Ternary Mixture Carbon Dioxide--Methyl Myristate--Methyl Palmitate. *Chem. Eng. Process.* **1994**, 33, 171 - 187.

(12) Bharath, R.; Inomata, H.; Arai, K.; Shoji, K.; Noguchi, Y. Vapor-Liquid Equilibria for Binary Mixtures of Carbon Dioxide and Fatty Acid Ethyl Esters. *Fluid Phase Equilib.* **1989**, 50, 315 - 327.

(13) Ferreira, O.; Macedo, E. A.; Brignole, E. A. Application of the GCA-EoS Model to the Supercritical Processing of Fatty Oil Derivatives. *J. Food Eng.* **2005**, 70, 579 - 587.

(14) Jaubert, J.; Coniglio, L. The Group Contribution Concept: a Useful Tool to Correlate Binary Systems and to Predict the Phase Behavior of Multicomponent Systems Involving Supercritical CO_2 and Fatty Acids. *Ind. Eng. Chem. Res.* **1999**, 38, 5011-5018.

(15) Byun, H.; Kim, K.; McHugh, M. A. Phase Behavior and Modeling of Supercritical Carbon Dioxide-Organic Acid Mixtures. *Ind. Eng. Chem. Res.* **2000**, 39, 4580-4587.

(16) Heo, J.; Shin, H. Y.; Park, J.; Joung, S. N.; Kim, S. Y.; Yoo, K. Vapor-Liquid Equilibria for Binary Mixtures of CO_2 With 2-Methyl-2-Propanol, 2-Methyl-2-Butanol, Octanoic Acid, and Decanoic Acid at Temperatures From 313.15 K to 353.15 K and Pressures From 3 MPa to 24 MPa. *J. Chem. Eng. Data* **2001**, 46, 355-358.

(17) Weidner, E.; Wiesmet, V.; Knez, Z.; Skerget, M. Phase Equilibrium (Solid-Liquid-Gas) in Polyethyleneglycol-Carbon Dioxide Systems. *J. Supercrit. Fluids* **1997**, 10, 139 - 147.

(18) Daneshvar, M.; Kim, S.; Gulari, E. High-Pressure Phase Equilibria of Polyethylene Glycol-Carbon Dioxide Systems. *J. Phys. Chem.* **1990**, 94, 2124-2128.

(19) Chang, C. J.; Lee, M.; Li, B.; Chen, P. Vapor-Liquid Equilibria and Densities of CO_2 With Four Unsaturated Fatty Acid Esters at Elevated Pressures. *Fluid Phase Equilib.* **2005**, 233, 56 - 65.

(20) Inomata, H.; Kondo, T.; Hirohama, S.; Arai, K.; Suzuki, Y.; Konno, M. Vapour--Liquid Equilibria for Binary Mixtures of Carbon Dioxide and Fatty Acid Methyl Esters. *Fluid Phase Equilib.* **1989**, 46, 41 - 52.

(21) Crampon, C.; Charbit, G.; Neau, E. High-Pressure Apparatus for Phase Equilibria Studies: Solubility of Fatty Acid Esters in Supercritical CO_2. *J. Supercrit. Fluids* **1999**, 16, 11 - 20.

(22) Carvalho, P. J.; Álvarez, V. H.; Machado, J. J. B.; Pauly, J.; Daridon, J.; Marrucho, I. M.; Aznar, M.; Coutinho, J. A. P. High Pressure Phase Behavior of Carbon Dioxide in 1-Alkyl-3-Methylimidazolium Bis(Trifluoromethylsulfonyl)Imide Ionic Liquids. *J. Supercrit. Fluids* **2009**, 48, 99-107.

(23) Carvalho, P. J.; Alvarez, V. H.; Marrucho, I. M.; Aznar, M.; Coutinho, J. A. P. High Pressure Phase Behavior of Carbon Dioxide in 1-Butyl-3-Methylimidazolium Bis(Trifluoromethylsulfonyl)Imide and 1-Butyl-3-Methylimidazolium Dicyanamide Ionic Liquids. *J. Supercrit. Fluids* **2009**, 50, 105-111.

(24) Carvalho, P. J.; Álvarez, V. H.; Marrucho, I. M.; Aznar, M.; Coutinho, J. A. P. High Carbon Dioxide Solubilities in Trihexyltetradecylphosphonium-Based Ionic Liquids. *J. Supercrit. Fluids* **2010**,

submitted.

(25) Anthony, J.; Anderson, J.; Maginn, E.; Brennecke, J. Anion Effects on Gas Solubility in Ionic Liquids. *J. Phys. Chem. B* **2005**, 109, 6366-6374.

(26) Anthony, J.; Maginn, E.; Brennecke, J. Solubilities and Thermodynamic Properties of Gases in the Ionic Liquid 1-N-Butyl-3-Methylimidazolium Hexafluorophosphate. *J. Phys. Chem. B* **2002**, 106, 7315-7320.

(27) Aki, S. N. V. K.; Mellein, B. R.; Saurer, E. M.; Brennecke, J. F. High-Pressure Phase Behavior of Carbon Dioxide With Imidazolium-Based Ionic Liquids. *J. Phys. Chem. B* **2004**, 108, 20355-20365.

(28) Vitu, S.; Jaubert, J. N.; Pauly, J.; Daridon, J. L.; Barth, D. Phase Equilibria Measurements of CO_2 + Methyl Cyclopentane and CO_2 + Isopropyl Cyclohexane Binary Mixtures at Elevated Pressures. *J. Supercrit. Fluids* **2008**, 44, 155-163.

(29) Pauly, J.; Coutinho, J.; Daridon, J. L. High Pressure Phase Equilibria in Methane + Waxy Systems: 1. Methane + Heptadecane. *Fluid Phase Equilib.* **2007**, 255, 193-199.

(30) Ventura, S. P. M.; Pauly, J.; Daridon, J. L.; da Silva, J. A. L.; Marrucho, I. M.; Dias, A. M. A.; Coutinho, J. A. P. High Pressure Solubility Data of Carbon Dioxide in Tri-Iso-Butyl(Methyl)Phosphonium Tosylate - Water Systems. *J. Chem. Thermodyn.* **2008**, 40, 1187-1192.

(31) Dias, A. M. A.; Carrier, H.; Daridon, J. L.; Pamies, J. C.; Vega, L. F.; Coutinho, J. A. P.; Marrucho, I. M. Vapor-Liquid Equilibrium of Carbon Dioxide-Perfluoroalkane Mixtures: Experimental Data and SAFT Modeling. *Ind. Eng. Chem. Res.* **2006**, 45, 2341-2350.

(32) Ventura, S. P. M.; Pauly, J.; Daridon, J. L.; Marrucho, I. M.; Dias, A. M. A.; Coutinho, J. A. P. High-Pressure Solubility Data of Methane in Aniline and Aqueous Aniline Systems. *J. Chem. Eng. Data* **2007**, 52, 1100-1102.

(33) Carvalho, P. J.; Álvarez, V. H.; Schröder, B.; Gil, A. M.; Marrucho, I. M.; Aznar, M.; Santos, L. M. N. B. F.; Coutinho, J. A. P. Specific Solvation Interactions of CO_2 on Acetate and Trifluoroacetate Imidazolium Based Ionic Liquids at High Pressures. *J. Phys. Chem. B* **2009**, 113, 6803-6812.

(34) Yokozeki, A.; Shiflett, M. B.; Junk, C. P.; Grieco, L. M.; Foo, T. Physical and Chemical Absorptions of Carbon Dioxide in Room-Temperature Ionic Liquids. *J. Phys. Chem. B* **2008**, 112, 16654-16663.

(35) Muldoon, M.; Aki, S.; Anderson, J.; Dixon, J.; Brennecke, J. Improving Carbon Dioxide Solubility in Ionic Liquids. *J. Phys. Chem. B* **2007**, 111, 9001-9009.

(36) Charoensombut-amon, T.; Martin, R. J.; Kobayashi, R. Application of a Generalized Multiproperty Apparatus to Measure Phase Equilibrium and Vapor Phase Densities of Supercritical Carbon Dioxide in N-Hexadecane Systems Up to 26 MPa. *Fluid Phase Equilib.* **1986**, 31, 89-104.

(37) Kumelan, J.; Pérez-Salado Kamps, Á.; Tuma, D.; Maurer, G. Solubility of CO_2 in the Ionic Liquid [Hmim][Tf_2N]. *J. Chem. Thermodyn.* **2006**, 38, 1396 - 1401.

(38) Kumelan, J.; Tuma, D.; Maurer, G. Solubility of CO_2 in the Ionic Liquids [Bmim][CH_3SO_4] and [Bmim][PF_6]. *J. Chem. Eng. Data* **2006**, 51, 1802-1807.

(39) Raeissi, S.; Peters, C. J. Carbon Dioxide Solubility in the Homologous 1-Alkyl-3-Methylimidazolium Bis(Trifluoromethylsulfonyl)Imide Family. *J. Chem. Eng. Data* **2009**, 54, 382-386.

(40) Gutkowski, K.; Shariati, A.; Peters, C. High-Pressure Phase Behavior of the Binary Ionic Liquid System 1-Octyl-3-Methylimidazolium Tetrafluoroborate + Carbon Dioxide. *J. Supercrit. Fluids* **2006**, 39, 187-191.

(41) Shariati, A.; Peters, C. J. High-Pressure Phase Equilibria of Systems With Ionic Liquids. *J. Supercrit. Fluids* **2005**, 34, 171-176.

(42) Tanaka, H.; Yamaki, Y.; Kato, M. Solubility of Carbon Dioxide in Pentadecane, Hexadecane, and Pentadecane + Hexadecane. *J. Chem. Eng. Data* **1993**, 38, 386-388.

(43) Maurer, G.; Kamps, A. P.. Developments and Applications in Solubility; : Letcher, T. M.; RSC Publishing, 2007; pp 41-58.

(44) Prausnitz, J. M.; Lichtenthaler, R. N.; Gomes de Azevedo, E. Molecular Thermodynamics of Fluid-Phase Equilibria; : Prentice Hall International Series: New York, 1999.